

Special Issue “Materiais 2015”

# Study of the viability of manufacturing ceramic moulds by additive manufacturing for rapid casting

Edwin Ocaña Garzón<sup>a,b\*</sup>, Jorge Lino Alves<sup>b</sup>, Rui J. Neto<sup>b</sup>

<sup>a</sup>*Departamento de Ciências de la Energía y Mecánica (DECEM), Universidad de las Fuerzas Armadas ESPE, Sangolquí, Ecuador*

<sup>b</sup>*INEGI, Faculty of Engineering, University of Porto, 4200-465, Porto, Portugal*

## Abstract

Additive manufacturing (AM) has been considered one of the best processes to manufacture components with complex geometries, many times impossible to achieve with traditional processes, such as moulds with conformal cooling. Binder Jetting (BJ) technology uses an ink-jet printing head that deposits an adhesive liquid, layer by layer, to bind a powder material that can be ceramic, metallic, or other, which allows manufacturing parts to be used in research and industry.

The aim of this work is to study the possibility of using BJ to produce plaster moulds for directly cast metallic parts at a lower cost than with metallic AM processes, using different types of infiltrates and post-processing parameters to improve the mechanical and thermal strength of moulds in order to be able to cast an aluminium alloy. The mechanical and thermal resistance of moulds with a thickness range of 2.5–4mm were analysed, as well as the surface roughness of metal samples, and compared with those obtained by traditional processes. Although all the moulds had good heat resistance during the casting, some did not have enough mechanical strength to withstand the metalostatic pressure, especially those with walls of 2.5 to 3.5 mm.

© 2017 Portuguese Society of Materials (SPM). Published by Elsevier España, S.L.U. All rights reserved.

*Keywords:* Additive manufacturing; 3D printing; rapid casting; plaster moulds.

## 1. Introduction

The ASTM International Committee F42 on Additive Manufacturing Technologies (AM) defined AM as the process of joining materials to make objects from 3D model data, usually layer upon layer [1] which is commonly known as 3D printing (3DP). This technology does not subtract material and has a wide field of applications, producing parts in minutes, hours or few days (depending on complexity) in different types of materials [2], and its main advantage is that it does not rely on the operator's ability to manufacture unimaginable parts.

Since 1987, when the first commercial AM System,

SLA-1, was launched by 3D Systems in USA [3], the growth of this industry has accelerated, with an increasing number of organizations adopting AM products and services. The compound annual growth rate (CAGR) of worldwide revenues produced by all products and services, over the past 26 years, is an impressive 27.3%. The CAGR from 2012–2014 is 33.8%. The market has nearly quadrupled in the last five years [1].

The first use of AM parts as sacrificial patterns in traditional investment casting (IC) started in 1989. Since then, all major AM techniques have been used in different casting methods to provide Rapid Investment Casting (RIC) solutions for producing metal parts, using direct and indirect conversion technologies [4–6].

IC allows the production of accurate components in low or high volumes as a competitive alternative to

\* Corresponding author.

E-mail address: [emocania@espe.edu.ec](mailto:emocania@espe.edu.ec)

forging or metal turning since the waste material is kept to a minimum [7].

The economic benefits derived from AM patterns are limited to small quantity production due to high AM material costs [8]. The choice of the AM technique to be used will depend on many factors such as shape, dimensional tolerances, the cost assigned to the model, among others [9].

The ProJet 660 Pro machine uses a ColorJet Printing (CJP) technology that consolidates a plaster-ceramic powder by selective jetting of a water based binder. Complex cores and cavities can be produced directly from the CAD model, completed with the gating system and air vents, avoiding the construction of patterns and core boxes [10]. Post-processing is a critical important aspect of 3D printing, but it is often overlooked or underemphasized in product literature and by the media. 3D printing requires specific knowledge and techniques to produce a “finished” part [1]. Typically, post-processing is needed to remove support material from parts by water jet, air jet, dissolution, or other mechanical process. In the ProJet 660 Pro (Fig. 1) the loose powder is removed with a brush and by air jet, and the part is posteriorly infiltrated with hardeners as cyanoacrylate, polymeric resins, or other material to increase the strength and brighten colours to get a functional component.



Fig. 1. a) Printed specimens; b) FEUP's ProJet 660 PRO Series machine.

This research has the following objectives:

- Feasibility of making moulds for casting aluminium by 3D printing, using the ProJet 660 Pro;
- The raw material is the one recommended by the manufacturer: calcium sulphate hemihydrate 80-90% (3D Systems USA) by selective jetting of water-based binder [11]. It is known that the binder does not support high temperatures, so the research will focus on finding adequate infiltrates, in the post-processing, to provide satisfactory results for a mould with enough

strength to withstand the casting of the selected aluminium alloy;

- Determine the tolerance and surface roughness of the castings.

## 2. Experimental work

### 2.1. CAD design

The experimental process began by defining a simple shape mould, as shown in Fig. 2. This geometry was initially adopted because the goal was to test different infiltrates to harden the mould. This geometry was modelled in 3D CAD software, and the internal dimensions were maintained, according to Fig. 2. Four different wall thicknesses were selected; 2.5, 3.0, 3.5 and 4.0 mm to evaluate mould resistance.

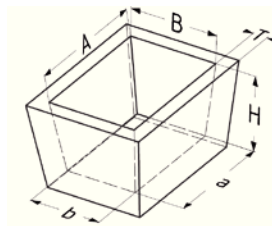


Fig. 2. Specimen shape used as mould.

### 2.2. AM of moulds

The CAD file was saved in a STL extension and later used along with the 3D Edit Pro 2.0 printer software; all the specimens were located in optimum position for printing. The samples were printed in different batches, and Table 1 specifies the main characteristics of the job, in terms of printing time and amount of powder and binder. It should be noted that although this printer has the possibility to print in colour, in this work, this feature was not necessary; thus, all the samples were printed in the monochrome mode, so the amount of binder basically reflects clear binder.

Table 1. Specimen printing characteristics: time, volume of powder and binder.

| Wall thickness (mm) | Build time; 12 samples (min) | Volume binder/part (mL) | Volume powder/part (cm <sup>3</sup> ) |
|---------------------|------------------------------|-------------------------|---------------------------------------|
| 2.50                | 77.94                        | 8.30                    | 8.20                                  |
| 3.00                | 82.78                        | 6.07                    | 10.29                                 |
| 3.50                | 82.78                        | 7.08                    | 12.01                                 |
| 4.00                | 87.00                        | 8.13                    | 14.31                                 |

Prior to impregnation, the internal dimensions were controlled with a Vernier (for each dimension, 3 measurements were made; extremities and middle, and the average value presented in Table 2), in 4 specimens of each thickness, randomly chosen. Table 2 also indicates the average deviation (relative to the expected CAD value), allowing to verify internal dimensional accuracy in printing, and compare it with other equipment of similar characteristics [12].

Table 2. Internal dimensions of green samples and difference relative to the CAD dimensions (mm).

|   | CAD dimension | Average size by wall thickness |       |       |       | Average | Average deviation |
|---|---------------|--------------------------------|-------|-------|-------|---------|-------------------|
|   |               | 2.5                            | 3.0   | 3.5   | 4.0   |         |                   |
| A | 35.00         | 34.94                          | 34.99 | 34.99 | 35.00 | 34.98   | 0.02              |
| B | 25.00         | 24.97                          | 24.98 | 25.03 | 24.96 | 24.99   | 0.02              |
| a | 30.00         | 30.15                          | 30.14 | 30.07 | 30.12 | 30.12   | 0.02              |
| b | 20.00         | 20.22                          | 20.10 | 20.03 | 20.09 | 20.11   | 0.05              |
| H | 20.00         | 20.48                          | 20.32 | 20.26 | 20.25 | 20.33   | 0.08              |

### 2.3. Impregnation

Moulds were impregnated during different times, by full immersion with six different infiltrates: ethyl silicate (Wacker, Germany), Levasil (AkzoNovel N.V., Sweden), Ludox SK (Grace Davison, USA), Aerodisp (Evonik Industries, Germany), Ticoat-N (Rement, USA) and Zirconium acetate (Nyacol Nanotech Inc., USA), which are typically used in ceramic block moulding and investment casting [13–15].

Table 3 does not present equal number of moulds infiltrated for each thickness since some of them were destroyed during the exploratory tests with different infiltrating times, due to the lower wall thickness.

Moulds were allowed to dry at room temperature with forced air for 2h. Table 3 indicates the conditions used for all samples. Specimens without infiltrate were also used to observe the behaviour of only the printer's binder. Three different cycles (first column) were employed to check the effect of heating temperature on moulds' behaviour. The identification of the specimens "iTxx" means that "i" is the No. of specimen (Table 3), and "Txx" corresponds to the wall thicknesses.

### 2.4. Mould heating and casting

The moulds were heat treated according to a recommended heating cycle for plaster moulds used in investment casting [16,17]. Three different cycles

were adopted as shown in Fig. 3; Ticoat-N and Zirconium Acetate infiltrates require sintering temperatures of 1100°C [18], and so are only considered in cycle 3.

Table 3. Specimen's specifications.

| Heat cycle n° | Spec. n° "i" | Wall thickness spec. (mm) "T" | Immersion time (s) | Type of infiltrate |
|---------------|--------------|-------------------------------|--------------------|--------------------|
| 1             | 1P           | 2.5                           | -                  | Without infiltrate |
| 2             | 1            | 3.0 ; 3.5                     | 120                | Ethyl silicate*    |
|               | 2            | 3                             | 5                  | Ethyl silicate     |
|               | 3            | 2.5 ; 3.0                     | 120                | Ethyl silicate     |
|               | 4            | 2.5 ; 3.5                     | 5                  | Levasil            |
|               | 5            | 2.5 ; 3.5                     | 5                  | Ludox SK           |
|               | 6            | 2.5 ; 3.5                     | 5                  | Aerodisp**         |
|               | 7            | 2.5 ; 3.5                     | 5                  | Aerodisp           |
|               | 8            | 3.5                           | -                  | -                  |
| 3             | 9            | 4.0                           | 10 ; 20            | Ludox SK           |
|               | 10           | 4.0                           | 10 ; 20            | Levasil            |
|               | 11           | 4.0                           | 10 ; 20            | Aerodisp           |
|               | 12           | 4.0                           | 10 ; 20            | Ticoat - N         |
|               | 13           | 4.0                           | 10 ; 20            | -                  |
|               | 14           | 4.0                           | 10 ; 20            | Zirconium acetate  |

\* Hydrolyzed (50% ethyl silicate + 50% isopropyl alcohol silicate)

\*\* 50% H<sub>2</sub>O

After each thermal cycle, the furnace was turned off and the samples allowed to cool to 450°C. The moulds were then removed and the aluminium alloy AlSi9Cu3 casted on them at 700°C [19]. This alloy was selected because was available in INEGI and is frequently used in foundry.

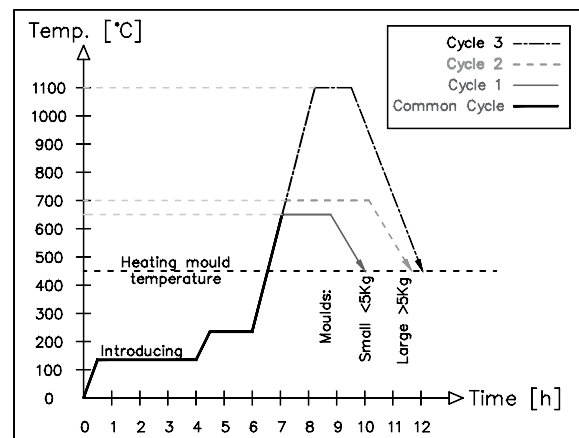


Fig. 3. Heating cycles of plaster moulds.

It should be referred that in cycles 2 and 3, at least two specimens were heated with each type of infiltrate. For each sample, one mould was kept unfilled to analyse

the friability (see Fig. 4 and Table 5).

### 2.5. Roughness test

The roughness measurement was only performed in aluminium parts submitted to cycle 3 because this cycle produced higher moulds resistance, which is a result of using thicker walls and the best infiltrates of cycle 2. Fig. 4 shows the surface quality of casted samples. The roughness was measured 3 times, in the directions indicated with arrows, in different regions of each face indicated on Fig. 4 (X–base, Y–long side, and Z–small side).

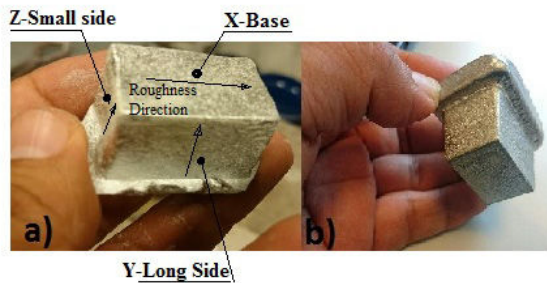


Fig. 4. Aluminium parts obtained from moulds: a) with infiltrate Ludox SK, and b) without infiltrating.

The values obtained are depicted on Table 6. The measurements on faces Y and Z were done perpendicular to the printing direction of the mould. In these directions, the roughness will be higher due to the printed layers orientation. The test was conducted in a length of 4.8 mm with a roughness meter “Hommel Werke”.

## 3. Results and Discussion

### 3.1. AM of moulds and impregnation

It should be noted that moulds were printed in different positions but all of them with the same orientation, so there will be no significant differences in their mechanical resistance, as demonstrated by J. Frascati [20].

It was observed that longer immersion times, maximum 120s (depending on type of infiltrate, since not all the infiltrates allowed to work with these times), gets greater penetration into the mould, but when this time is too long, it produces a surface softening, with the consequent complication in handling.

After casting and infiltrating tests, it was possible to evaluate the thickness stability. The 4 mm wall thickness specimens kept their integrity during the

casting independently of the immersion time.

Table 4 indicates the dimension control after impregnation. It presents the results of moulds that kept their integrity to cast aluminium. Fig. 5 shows the average size of the specimens indicated in Table 4, before and after impregnation. These results are relative to the second heat cycle, where most of the infiltrates were used.

It is evident, in terms of dimensional stability, that sample 1T30 in general is the best one. For example, specimen 7T3.5 (specimen n° 7 and wall thickness 3.5 mm, immersed in AERODISP®) experienced mould shrinkage, and specimen 3T2.5 immersed in pure silicate (120s in ethyl silicate) exhibited some growth.

Table 4. Internal dimensions of the moulds after impregnation (mm).

| Mould dimension | Identification of specimens |       |       |       |       |       |
|-----------------|-----------------------------|-------|-------|-------|-------|-------|
|                 | 1T3.0                       | 3T2.5 | 4T2.5 | 5T2.5 | 5T3.5 | 7T3.5 |
| A               | 34.99                       | 35.02 | 34.96 | 35.21 | 35.10 | 34.99 |
| B               | 25.02                       | 25.07 | 25.05 | 25.07 | 24.91 | 24.90 |
| A               | 30.10                       | 30.17 | 30.05 | 30.01 | 29.86 | 30.05 |
| B               | 20.20                       | 20.18 | 19.93 | 20.03 | 19.97 | 20.04 |
| H               | 20.27                       | 20.26 | 20.37 | 20.35 | 20.26 | 20.27 |

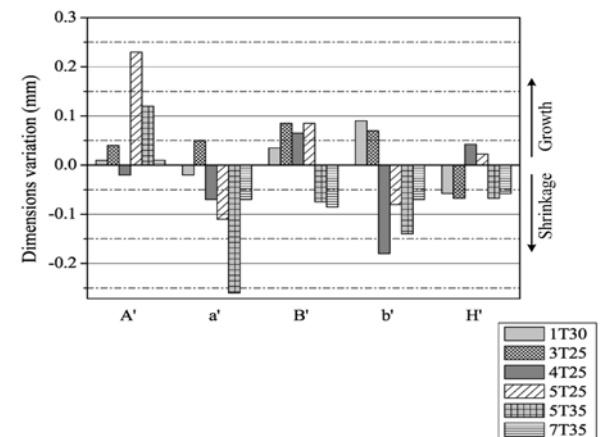


Fig. 5. Variation of the internal dimensions in specimens after impregnation (heating cycle 2).

### 3.2. Mould heating and casting

During casting, some problems occurred with the samples submitted to cycle 2: the height of the crucible relatively to the small moulds originated high metal impact that contributed to moulds fracture (Fig. 6). Considering this problem, for cycle 3, the moulds were enclosed with ceramic plates, the size of the crucible was reduced as well as the same height was set at 150 mm, and the mould wall thickness was

increased to 4 mm; this contributed to achieve better results as shown in Fig. 6.



Fig. 6. Moulds submitted to heat treatment: a) cycle 1, b) cycle 2 and c) cycle 3, after casting.

Table 5 indicates a friability property that uses an arbitrary scale, with values from 1 to 8, where 1 was assigned to the specimen with better consistency and 8 to the worst.

Table 5. Post-processing moulds condition.

| Heat cycle n° | Spec. n° | Type of infiltrate | Infiltrate penetration after treatment | Friability |
|---------------|----------|--------------------|--|------------|
| 1             | 1P       | Without infiltrate | -                                      | 4          |
|               | 1        | Ethyl silicate*    | poor                                   | 6          |
|               | 2        | Ethyl silicate     | poor                                   | 7          |
|               | 3        | Ethyl silicate     | poor                                   | 8          |
|               | 4        | Levasil            | fair                                   | 2          |
| 2             | 5        | Ludox SK           | good                                   | 1          |
|               | 6        | Aerodisp**         | poor                                   | 3          |
|               | 7        | Aerodisp           | poor                                   | 4          |
|               | 8        | Without infiltrate | -                                      | 6          |
| 3             | 9        | Ludox SK           | fair                                   | 5          |
|               | 10       | Levasil            | fair                                   | 6          |
|               | 11       | Aerodisp           | poor                                   | 3          |
|               | 12       | Ticoat - N         | good                                   | 1          |
|               | 13       | Without infiltrate | -                                      | 7          |
|               | 14       | Zirconium acetate  | poor                                   | 8          |

\* Hydrolyzed (50% ethyl silicate + 50% isopropyl alcohol silicate)

\*\* 50% H<sub>2</sub>O

### 3.3. Roughness

Table 6 and Fig. 7 show the average roughness “Ra” obtained on faces X, Y and Z of aluminium specimens, with their respective standard deviations. These values are also compared with the average roughness of some other casting processes, namely

investment casting CLA (counter-gravity low-pressure casting of air-melted alloys) or CLV (counter-gravity low-pressure casting of vacuum-melted alloys) with Ra=2.4 mm [21,22], and shell moulding casting with Ra=2.9 mm [22].

Table 6. Average roughness “Ra” of the specimens (µm).

| Sample n° | 9        | 10             | 11            | 12             | 13                   | 14                |               |
|-----------|----------|----------------|---------------|----------------|----------------------|-------------------|---------------|
|           | Ludox SK | Levasil        | Aerodisp      | Ticoat-N       | Without infiltrating | Zirconium acetate |               |
| Side      | X        | 10.17<br>±2.02 | 7.99<br>±0.53 | 11.10<br>±1.06 | 10.33<br>±2.85       | 12.34<br>±0.75    | 9.88<br>±9.88 |
|           | Y        | 9.73<br>±0.76  | 7.88<br>±1.35 | 7.84<br>±1.23  | 9.64<br>±1.48        | 7.26<br>±2.15     | 3.24<br>±0.71 |
|           | Z        | 6.94<br>±0.40  | 5.96<br>±0.81 | 7.47<br>±1.19  | 7.05<br>±1.04        | 6.28<br>±0.61     | 5.10<br>±1.26 |

In analysing the roughness of each side, Fig. 7 shows that Z-small side has less roughness, while the side offering greater roughness is X-base, and the Y-long side shows an intermediate roughness against other sides. So, for each side, the standard deviations of the roughness of different infiltrates intersect among them, which indicates, first hand, that there is no significant statistical influence of the type of infiltrate on the response of surface roughness. However, on the Y-long side, Zirconium Acetate is statistically significant.

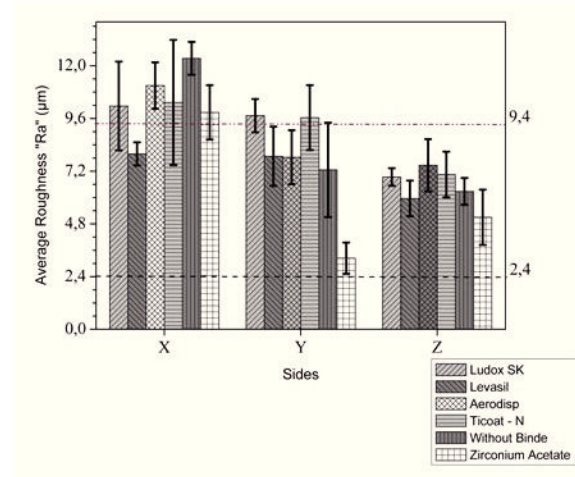


Fig. 4. Average roughness and their standard deviations of the aluminium specimens - Ra (µm).

### 4. Conclusions

All infiltrated moulds, reached a suitable thermal resistance to withstand the casting since none of them presented the visual sign of inflammation or burn. The mechanical resistance of the moulds was not enough to withstand the pressure of molten metal,

especially in the wall of thickness from 2.5 to 3.5 mm. However, best results are achieved with Ludox SK, Ticoat-N, Levasil and Aerodisp, infiltrating with friability scale with designation of 1, 1, 2 and 3, respectively.

The roughness Ra is not statistically significant according to the infiltrating, with the exception being the Zirconium acetate, on the Y-Long side; X-Base is found to have the worst roughness when compared with the other faces, whereas, the Z-Small side shows the best surface roughness. This analysis also revealed that aluminium parts in almost all the cases found to be within the range of roughness, which are obtained with the traditional processes of foundry, *viz.* investment casting CLA/CLV and shell mould casting. Behaviour of infiltrated moulds, when they are heated during cycle 3, did not improve the strength of mould, as the plaster above 1000°C changes to insoluble anhydrite at temperature in the range 380-1180°C [23]; so, it has no significance on the sinter of the infiltrating that was intended to give in this heat cycle. Future work can be routed to search new infiltrating types that can support high temperature and also can be subjected to thermal cycles with lower temperatures.

### Acknowledgements

Authors gratefully acknowledge funding of Project to Universidad de las Fuerzas Armadas ESPE, and SAESCTN-PII&DT/1/2011 co-financed by Programa Operacional Regional do Norte (ON.2 – O Novo Norte), under Quadro de Referência Estratégico Nacional (QREN), through Fundo Europeu de Desenvolvimento Regional (FEDER).

### References

[1] Wohlers Associates, Wohlers Report 2015, 3D Printing and AM State of the Industry, Annual Worldwide Progress Report, 20th ed., Wohlers Associates Inc., Colorado, USA, 2015.  
 [2] D.P.C. Velazco, E.F. Sancet, F. Urbaneja, M. Piccico, M.F. Serra, M.F. Acebedo, N.M. Rendtorff, *Ceramica* 60 (2014) 465.

[3] S.C.K. Chua, K.F. Leong (Ed.), *3D Printing and Additive Manufacturing*, 4th. ed., World Scientific Publishing. Co. Pte. Ltd., Singapore, 2015.  
 [4] M. Chhabra, R Singh, *Rapid Prototyping J.* 328 (2011) 350.  
 [5] V. Csaky, R.J. Neto, T.P. Duarte, J.L. Alves, A framework for custom design and fabrication of cranio-maxillofacial prostheses using investment casting, in *Engineering Optimization IV*, Rodrigues *et al.* (Ed.), Taylor & Francis Group, London, UK, 2015, pp. 941-945.  
 [6] F. Lino, P. Ala, R. Neto, B. Paiva, R. Paiva, R. Sousa, *Proceedings of VRAP2003 - 1st International Conference on Advanced Search in Virtual and Rapid Prototyping*, Leiria, Portugal, October 1-4, 2003, pp. 517-524.  
 [7] C. Yuan, S. Jones, *J. Eur. Ceram. Soc.* 23, (2003) 399.  
 [8] C.M. Cheah, C.K. Chua, C.W. Lee, C. Feng, K. Totong, *Int. J. Adv. Des. Manuf. Technol.* 25 (2004) 308.  
 [9] T.M. Duarte, *Fabrico rápido de ferramentas por fundição de precisão*, Repositorio FEUP/DEMEGI, 2002.  
 [10] E. Bassoli, A. Gatto, L. Iuliano, MG. Violante, *Rapid Prototyping J.* 13 (2007) 3.  
 [11] I. Gibson, D. Rosen, B. Stucker, *Binder Jetting*, in *Additive Manufacturing Technologies 3D Printing, Rapid Prototyping, and Direct Digital Manufacturing*, Springer, New York, 2015, pp. 205-218.  
 [12] M. Asadi-Eydivand *et al.*, *Rob. Comput. Integr. Manuf.* 37 (2015) 57.  
 [13] S. Pattnaik, D.B. Karunakar, P.K. Jha, *J. Mater. Process. Technol.* 212 (2012) 2332.  
 [14] B. Previtali, D. Poggi, C. Taccardo, *Composites, Part A* 39 (2008) 10.  
 [15] N. Yadav *et al.*, *International Journal of Emerging Technology and Advanced Engineering* 3 (2013), 543.  
 [16] J. Nunes, MSc thesis, Faculdade de Engenharia da Universidade do Porto, Porto, Portugal, 1999.  
 [17] J.P. Costes, M. Bigerelle, A. Iost, *Sci. Arts Métiers* (2007).  
 [18] Yuan, C., X. Cheng, and P.A. Withey, *Mater. Chem. Phys.* 155 (2015) 205.  
 [19] V.D. Tsoukalas, *Mater. Des.* 29 (2008) 10.  
 [20] J. Frascati, MSc thesis, Department of Mechanical Materials and Aerospace Engineering, University of Central Florida, Florida, USA, 2007.  
 [21] I. Gibson, D. Rosen, B. Stucker (Ed.), *Additive Manufacturing Technologies: 3D Printing, Rapid Prototyping, and Direct Digital Manufacturing*, Springer New York, USA, 2014.  
 [22] M.F. Ashby, *Materials Selection in Mechanical Design*, 4th ed., E. Butterworth-Heinemann-Elsevier Science, Oxford, UK, 2011.  
 [23] R.A. Kuntze (Ed.), *Gypsum: Connecting Science and Technology*, ASTM International, USA, 2009.